



# Performance assessment of wood, metal and composite baseball bats

Mahesh M. Shenoy, Lloyd V. Smith <sup>\*</sup>, John T. Axtell

*School of Mechanical and Materials Engineering, Washington State University, Pullman, WA, USA*

---

## Abstract

The purpose of this investigation was to develop and verify a predictive capability of determining baseball bat performance. The technique employs a dynamic finite element code with time dependent baseball properties. The viscoelastic model accommodates energy loss associated with the baseball's speed dependent coefficient of restitution (COR). An experimental test machine was constructed to simulate the ball–bat impact conditions in a controlled environment and determine the dynamic properties of the baseball. The model has found good agreement with the experimental data for a number of impact locations, impact speeds, bat models and ball types. The increased hitting speed generally associated with aluminum bats is apparent, but not for impacts inside of the sweet spot. A reinforcing strategy is proposed to improve the durability of wood bats and is shown to have a minimal effect on its hitting performance. The utility of using a constant bat swing speed to compare response of different bat types is also discussed. © 2001 Elsevier Science Ltd. All rights reserved.

**Keywords:** Baseball; Bat; Coefficient of restitution; Composite handle

---

## 1. Introduction

A number of popular sports have benefited from extensive research on sporting equipment, including racquet sports (such as tennis and badminton) and club sports (such as golf, cricket and baseball). Advanced composite materials are often used to reduce the weight and increase the durability of sports equipment. These materials may also allow the ball to be hit farther and with greater accuracy. The effect of technology on baseball has been significant, where modern aluminum and composite bats may hit a ball an average of 1 m/s (4 mph) faster than a traditional wooden bat [1]. Unlike most other sports, however, improvement in bat performance has been shunned at the professional level. Historically, the motivation for restricting bat performance was to assure fairness between hitters. Recent motivation appears centered around maintaining a competitive balance between the pitcher and the batter. This balance is real, as rookie players often require numerous seasons to adjust to wood bats. This adjustment has not gone unnoticed among amateur leagues and associations. The NCAA, for instance, has recently

adopted rules designed to limit the performance of non-wood bats [2].

The assessment of bat performance is a non-trivial matter and depends on many factors that are difficult to quantify or control. In the following, bat performance is taken to mean the hit speed of a baseball that is achieved after being pitched toward a swinging bat. The motion of a bat swing is complex, three dimensional, involves translation and rotation, and is difficult to replicate experimentally. A simulation only requires replicating the bat motion during the instant of contact with the ball, however, which primarily involves pure rotation [3].

The accuracy of bat performance predictions using closed form solutions has been limited by energy losses occurring during the bat–ball collision. Energy dissipation occurs primarily through surface contact friction, inelastic ball deformation, and elastic bat vibration. These losses are typically lumped together into a coefficient of restitution (COR) that is usually considered constant. The current study will show that these losses are not constant and vary with the relative speed of the ball and bat and the impact location of the ball with the bat.

Bat performance is currently assessed through experimental testing. The tests are expensive, time consuming and impede the design process. The primary objective of this paper is to develop a predictive technique of assessing bat performance. The technique is intended to be general and rigorous, allowing parameters controlling bat

---

<sup>\*</sup> Corresponding author.

E-mail address: [smith@mme.wsu.edu](mailto:smith@mme.wsu.edu) (L.V. Smith).

performance to be examined and manipulated in-house before fabricating and testing prototypes. (As an application of this technique, the effect of reinforcing a wooden bat on performance is examined.) The good agreement between the computational model and experimental results suggests this technique has potential in assisting the bat design process.

## 2. Bat testing machine

A bat test machine has been constructed to verify the computational model by experimentally determining the hitting performance and durability of a baseball bat in a controlled environment. In this arrangement, a swinging bat strikes a pitched ball as shown in Fig. 1. The balls are pitched using a two-wheel, counter-rotating pitching machine. The pitching machine is placed close to the bat to increase the pitch accuracy. The bat is supported by two rubber grips, which are in turn held in a steel fixture. The bat swings on a fixed axis. The bat center of rotation is adjustable, but nominally set at 75 mm (3 in.) from the knob and off the bat as indicated. This location was found to be the most common center of rotation at impact from an extensive study of amateur and professional players [3]. A pneumatic cylinder connected to a rack and pinion drives the bat. The swing speed of the bat is adjusted by changing the pressure in the cylinder. The timing of bat deceleration and ball pitch is accomplished through a series of non-contact electronic switches and a programmable logic controller. A torque cell and potentiometer in the load train allow bat torque, position and speed to be recorded for each test.

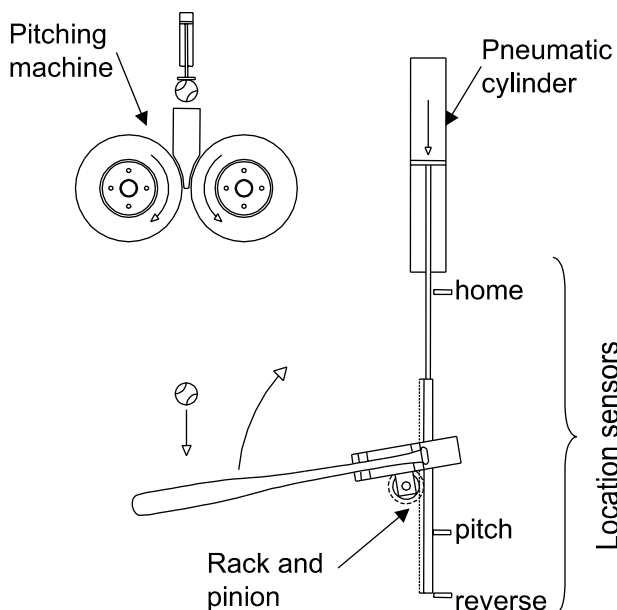


Fig. 1. Diagram of bat testing machine.

## 3. Material

The reliability of any predictive model is dependent on the accurate description of the materials involved. This becomes especially difficult when the materials are non-homogeneous, as observed in baseballs and wood bats.

### 3.1. Bats

In this study two primary bat materials are considered: wood and aluminum. The bats used for testing and analysis were all 860 mm (34 in.) long. The center of mass, weight and moment of inertia about the center of rotation for each bat type may be found in Table 1. In an effort to improve the durability of the wood bat, a reinforcing sleeve was placed over its handle. This bat is referred to as 'reinforced' in Table 1, where a unidirectional e-glass sleeve has been used. Reinforcing the wooden bat with a composite sleeve had little effect on its inertia but the center of mass shifted toward the knob end by 10–15 mm (0.40–6 in.) depending on the reinforcement used. The properties of wood can vary widely within and especially between species. Nominal orthotropic properties of Northern White Ash were used, as statistical variation in material properties was not an aim of this study. These were obtained experimentally and corroborated with accepted values [4,5]. While aluminum bats are usually alloyed, this does not affect their elastic response appreciably [6]. The properties of the wood, aluminum and two reinforcing materials used in the computational model are presented in Table 2.

### 3.2. Balls

Two types of balls have been considered in this study. The first is a traditional baseball, produced from yarn wound around a cork and rubber pill, and covered with leather. The second baseball type is synthetic and commonly used in batting cages. It is injection molded from an air filled rubber and designed to simulate the hitting characteristics of a traditional baseball. Several attempts were made to extract the elastic properties of the baseball through quasi-static compression testing. These included compression loading a baseball between flat platens and comparing the load displacement curve with a large deflection Hertzian type contact model [7]. For

Table 1  
Bat mass and inertia properties

Bat	Mass (g)	C.G. (mm)	Inertia ( $\text{kg m}^2$ )
Ash	845	580	0.255
Reinforced	887	565	0.257
Aluminum	845	567	0.254

Table 2

Elastic properties of bat materials (GPa)

Material	$E_1$	$E_2$	$E_3$	$G_{12}$	$G_{23}$	$G_{13}$	$v_{12}$	$v_{23}$	$v_{13}$
Ash	13.9	1.33	1.47	1.23	0.14	0.83	0.4	0.5	0.5
Aluminum	70.5	70.5	70.5	27.1	27.1	27.1	0.3	0.3	0.3
e-glass/epoxy	42.7	9.30	9.30	4.70	3.40	4.70	0.25	0.35	0.25
Carbon/epoxy	102	7.20	7.20	3.60	2.70	3.60	0.31	0.35	0.31

the case of the homogeneous synthetic ball a uniaxial compression specimen was cut from the ball. The elastic modulus was then found from the compressive stress-strain response of this coupon. In both cases, however, the elastic modulus was apparently too low. This was determined by examination of deformation patterns from numerical impact simulations. It was postulated that the disparate strain rates achievable with a load frame and that occurring in an actual ball–bat impact (roughly three orders of magnitude) may be significant. Thus a time dependent material model and a high load rate testing device were needed.

A viscoelastic material model was selected for the ball, defined from a time dependent shear modulus as formulated by Hermann and Peterson [8] as

$$G(t) = G_\infty + (G_0 - G_\infty)e^{-\beta t} \quad (1)$$

and a constant bulk modulus,  $k$ . According to Eq. (1),  $G_0$  may be viewed as the instantaneous modulus at  $t = 0$ , while  $G_\infty$  is the fully relaxed modulus at  $t = \infty$ . The magnitude of  $\beta$  determines the time sensitivity of the model. A high strain rate was experimentally achieved by pitching baseballs at a rigidly mounted load cell. This impact was simulated using the numerical model. The

constants  $G_0$ , and  $\beta$  were found by fitting the experimental load-time curve with that obtained from the finite element analysis, while the fully relaxed modulus,  $G_\infty$ , was found from the quasi-static testing. A comparison of these curves is presented in Fig. 2 for the case of a synthetic baseball pitched at  $v_p = 49$  m/s (110 mph). Effective material properties for the two ball types (traditional and synthetic) may be found in Table 3 [9]. Unless indicated otherwise, the remaining comparisons contained in this work have been performed using a traditional baseball.

### 3.3. Composite reinforcement

The most common location of failure for wood bats is a region extending from 250 to 500 mm (10–20 in.) from the knob end of the bat. It was proposed that a lightweight fiber reinforced grip in this region would make the bat more durable. Two types of reinforcements were considered, namely carbon and e-glass fiber in unidirectional and braided orientations.

The properties for these reinforcements were found using the rule of mixtures (50% volume fraction) and a three dimensional lamination theory [10,11]. The nominal geometry of the braided sleeves are shown in Table 4 while the unidirectional elastic properties of the fiber reinforced composite were presented in Table 2. The changing profile of the bat along its length affects the thickness of the reinforcement sleeves and the fiber orientation of braided sleeves. For the unidirectional sleeve, its thickness,  $t_u(x)$ , is a function of only the bat diameter,  $d(x)$ , which can be expressed as

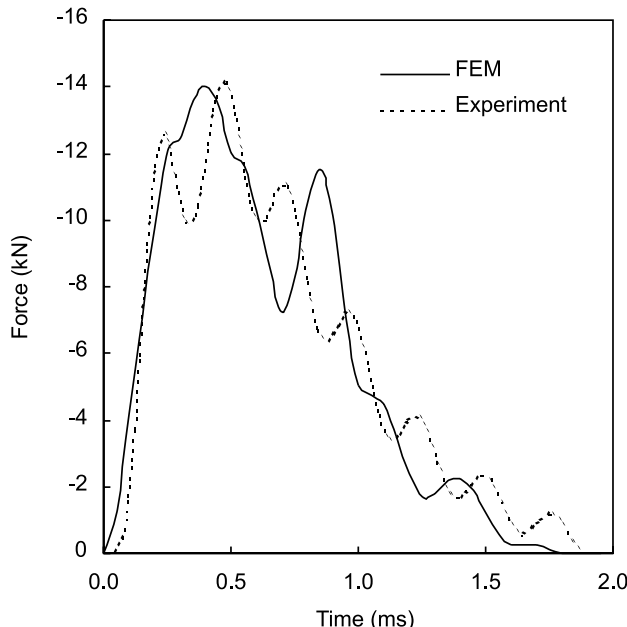


Fig. 2. Comparison of finite element results and experiment of a synthetic baseball impacting a load cell at  $v_p = 49$  m/s (110 mph).

Table 3  
Viscoelastic properties of two baseballs

Ball type	$G_0$ (MPa)	$G_\infty$ (MPa)	$\beta$	$k$ (MPa)
Traditional	31	10	11 000	93
Synthetic	2	1	1250	19

Table 4  
Nominal geometric properties of the reinforcing sleeves

Fiber type	Diameter (mm)	Thickness (mm)	Angle (deg)
e-glass	35	0.60	0
e-glass	51	0.28	±45
Carbon	38	0.58	0

$$t_u(x) = \frac{V}{L\pi d(x)} = \frac{d_0 t_0}{d(x)}, \quad (2)$$

where  $d_0$  and  $t_0$  are the nominal sleeve diameter and thickness, respectively, (Table 4), and  $V$  is the sleeve volume at an arbitrary length  $L$ . Since the unidirectional sleeve length,  $L$ , does not change with bat diameter, it is constant and cancels out.

For the braided sleeve, the thickness of the reinforcement is a function of the bat diameter,  $d(x)$ , as well as the braid angle,  $\theta(x)$ , which in turn depends on the bat diameter. The dependence of the braid angle on the bat diameter may be found by considering the braid as a flat surface as shown in the left of Fig. 3, or

$$\theta(x) = \sin^{-1} \left( \frac{\pi d(x)}{h} \right), \quad (3)$$

where  $h$  is found from the nominal angle and diameter of the braid.

If it is assumed that braid yarns do not slide relative to adjacent yarns, a unit cell of the braid architecture can be constructed as shown in the right of Fig. 3. The fiber length,  $l$ , is constant and the volume of the unit cell

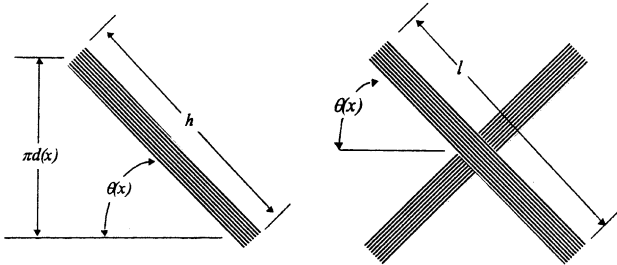


Fig. 3. Left: braid angle,  $\theta(x)$ , as a function of bat diameter,  $d(x)$ ; right: constant volume unit cell of a braided sleeve.

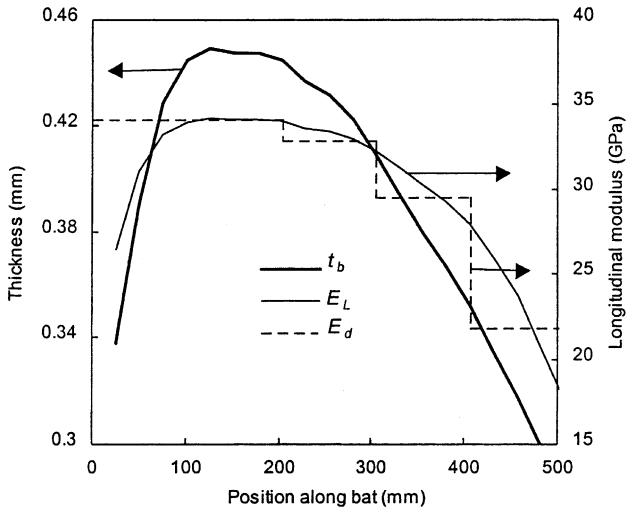


Fig. 4. The dependence of thickness and modulus of a braided reinforcement along the length of the bat.

(or quantity of fiber) is conserved. The thickness of the braided sleeve,  $t_b(x)$ , at a diameter  $d(x)$  and orientation  $\theta(x)$  is then found by equating the volume of its unit cell with that of the given nominal geometry and solving for  $t_b(x)$  as

$$t_b(x) = \frac{V}{l^2 \cos(\theta(x)) \sin(\theta(x))}, \quad (4)$$

where

$$\frac{V}{l^2} = t_0 \cos(\theta_0) \sin(\theta_0). \quad (5)$$

The effect of bat diameter on the reinforcement thickness,  $t_b$ , and longitudinal elastic modulus,  $E_L$ , is shown in Fig. 4, for a braided e-glass sleeve.

#### 4. Model description

The dynamic interactions of the bat and ball were modeled using a commercial dynamic finite element code, LS-Dyna 3D version 950 (Livermore Software Technology, Livermore, CA). All the analyses were performed on a 600 MHz Pentium III processor. The model consisted of 2048 and 9696, 8-noded solid elements for the ball and wooden bat, respectively, as shown in Fig. 5. The aluminum bat was meshed using 2496, 4-noded Hughes Liu shell elements which were used to support out of plane displacements and provide improved compatibility with solid elements [12]. The reinforced sleeve was also meshed using the 4-noded Hughes Liu shell elements. While these elements can accommodate shell thickness changes, the preprocessor used to generate the model did not. The sleeve was, therefore, discretized into four regions, where mean values for the thickness and modulus of each region were used. The discretized longitudinal modulus,  $E_d$ , used for the braided e-glass sleeve is shown in Fig. 4.

The effect of bat reinforcement was experimentally assessed from a static three point bend test and compared with an analytical model. The experimental test consisted of a 70 kg (150 lb) force applied centrally between supports 560 mm (22 in.) apart. The support on

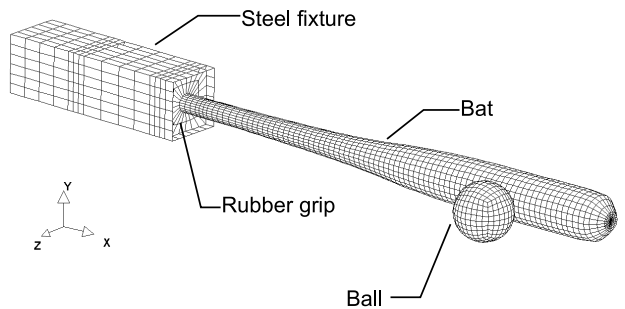


Fig. 5. Numerical model of the experimental set-up.

Table 5

Bat three point bend displacements (mm)

Bat	Experiment	Predicted	
		Continuous	Discrete
Ash	2.50	2.51	—
Reinforced	2.07	2.15	2.16
Aluminum	1.98	2.22	—

the handle region was 150 mm (6 in.) from the knob end of the bat. The stiffening effect on the bat reinforced with a braided e-glass sleeve is shown in Table 5, where the center-point displacement (averaged from 6 bats) is observed to decrease by 17%.

The bat center-point displacement was analytically computed by numerically fitting the bat profile and integrating along its length using Castiglano's method [13]. Center point displacement for continuously varying and discretized modulus (Fig. 4) are presented in Table 5. The good agreement with the experimental results suggests that the discretization technique employed in the finite element method is justified. There was some uncertainty concerning the wall thickness of the aluminum bat, however, which may be the cause of its poorer displacement correlation in Table 5.

A surface-to-surface contact between the bat and ball was accomplished using sliding contact elements that accounted for static and dynamic friction. These effects were small for the current study, however, as only normal impacts were considered. The explicit solution was obtained through iteration, where the solution time step was determined by an algorithm in the code that used the relative stiffness of the contacting surfaces. The bat was given an initial rotational velocity and the ball was pitched with an initial translational velocity (without rotation) normal to the length of the bat and in its swinging plane.

## 5. Experimental correlation

Dynamic experimental verification of the computational technique described above was accomplished by modeling the test cases performed on the bat testing machine and comparing the results. Comparisons of hit-ball speeds versus impact location were conducted for wood and reinforced bats. The reinforcement selected for experimental comparison was a unidirectional glass sleeve, 460 mm (18 in.) long. The bat swing speeds,  $v_s$ , used for the comparison were 22 and 13 m/s (50 and 30 mph), measured at 150 mm (6 in.) from the barrel end of the bat. The bats used here were 15% heavier than those listed in Table 1. Relatively slow speeds were used in this comparison, therefore, to prevent the premature failure of the heavier bats. The hit-ball speed,  $v_h$ , versus bat impact location has been plotted in Fig. 6. The numerically obtained hit-ball speeds correlate well with those

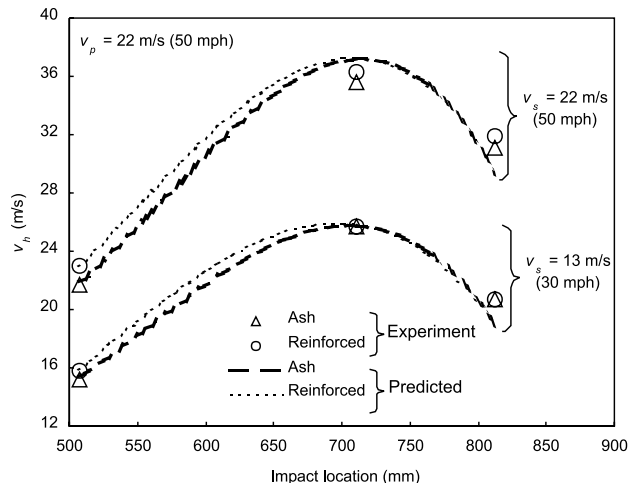


Fig. 6. Effect of impact location on hit-ball speed, experiment and predictions.

obtained experimentally. It should be noted that the post impact ball speed varies parabolically with bat impact location and is highest at around 700 mm (28 in.) from the knob of the bat. As will be shown later, this is not necessarily the bat's center of percussion (COP).

## 6. Hitting performance

There is clearly a paucity of rigorous scientific studies done on bat-ball impact and performance. Studying the effects of relative ball speed, bat geometry, bat inertia, etc. will facilitate a better understanding of the bat behavior.

### 6.1. Ball type

Bat performance is clearly dependent on the properties of the baseball. Slight differences exist among various brands of the traditional baseball. Synthetic balls (used for their increased durability in batting cages) can differ substantially from traditional balls, however, and are compared in Fig. 7 using a wood bat to illustrate extreme performance differences. For the case considered in Fig. 7, a synthetic ball is observed to perform similar to a traditional ball for inside hits yet performs significantly lower for outside impacts. (Here "inside" refers to locations between the knob end of the bat and the sweet spot, while "outside" refers to locations between the sweet spot and barrel end of the bat.) This trend is apparently due to a higher rate dependent energy dissipation of the rubber in the synthetic ball. The lower stiffness found in synthetic balls also leads to lower loads imparted to the bat. This has relevance in studies considering bat durability [14].

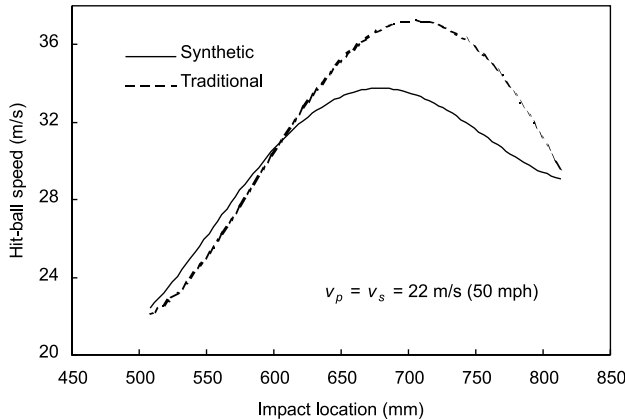


Fig. 7. Comparison of hit-ball speed for a traditional and synthetic baseball as a function of impact location.

## 6.2. Bat material

The hitting characteristics of a baseball bat are determined from its geometry and material. Once these are determined, other relevant properties such as mass, inertia and COP may be found. In the following, the three bat designs described in Table 1 are compared, where a unidirectional e-glass reinforcement was selected. A density of  $0.64 \text{ g/cm}^3$  was used for Ash [4,5], which provided similar weights and inertia between the bats.

A comparison of the hit-ball speed versus impact location for the three bat types is presented in Fig. 8. The reinforcement seems to have a negligible effect on the hit-ball speed of wood except for very inside hits, where it is slightly higher. The aluminum bat, however, shows a marked increase in hit-ball speeds, particularly for outside hits. Its sweet spot also appears to be 25 mm (1 in.) closer to the barrel end of the bat than wood. Interestingly, the advantage of aluminum is not apparent for inside hits, and even appears lower than wood at

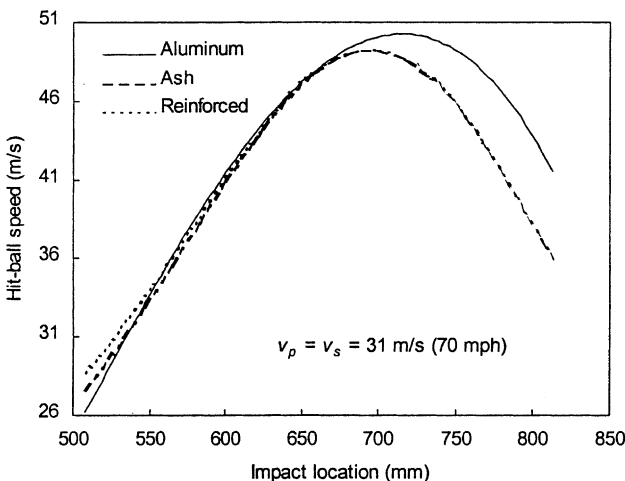


Fig. 8. Comparison of hit-ball speed with impact location for three bat types.

an impact location of 500 mm (20 in.) from the knob. This is likely due to the increased thickness to diameter ratio that occurs in aluminum as the barrel tapers into the handle. Low thickness to diameter ratios are generally thought to provide a “trampoline effect” in aluminum bats providing higher hit-ball speeds, as will be described in Section 6.3.

## 6.3. Bat performance metrics

The numerical model was used to examine the contact force between the ball and the aluminum bat described in Table 1 ( $t = 3 \text{ mm}$ ) as shown in Fig. 9. To study the effect of wall thickness, it was varied for bats of identical profile (with an associated change in inertia and weight) and compared in the figure. The maximum impulsive force (which affects bat durability) is shown to increase with wall thickness. In contrast to the maximum force, however, the impulse or area under the curve (which determines hit-ball speed) depends on the basis of comparison.

The mass and inertia properties of a bat are typically not regarded when assessing bat response. Current testing protocols, for instance, are designed to assure that bat and ball speeds remain constant for comparison [2,16]. To illustrate the significance of bat inertia on the performance basis, hit-ball speed has been plotted versus wall thickness of an aluminum bat in Fig. 10. The dotted line represents bats swinging at a constant speed of 31 m/s (70 mph) (measured at 150 mm from the end). Comparing on this constant swing speed basis, one might conclude that increasing the wall thickness of an aluminum bat would result in an increased hit-ball speed. This may be readily verified in experiments where

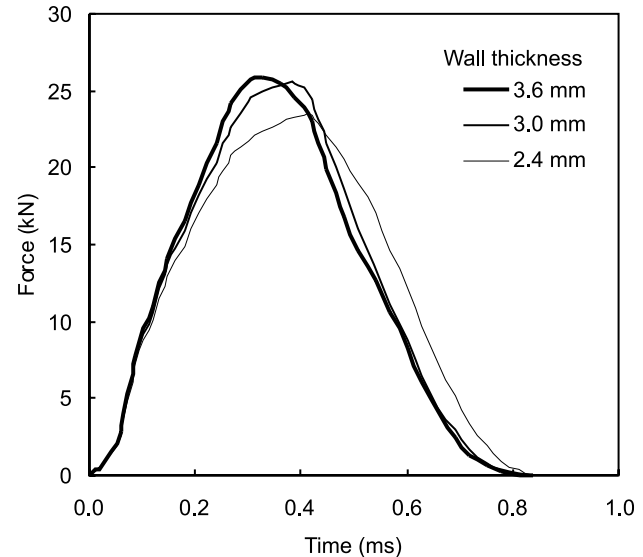


Fig. 9. Impact force versus time for an aluminum bat with increasing wall thickness.

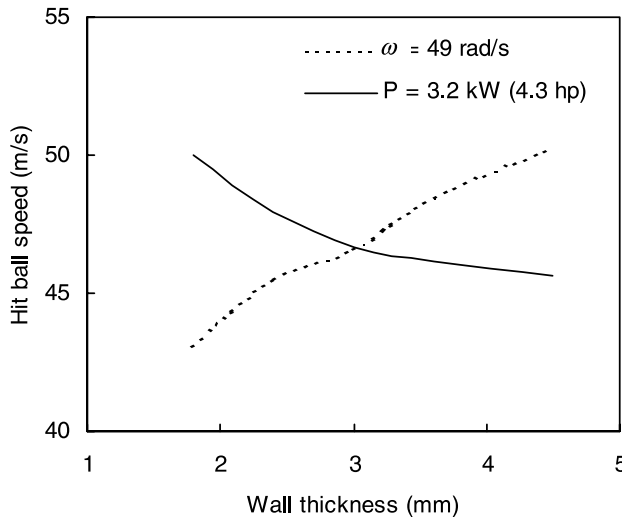


Fig. 10. Hit-ball speed comparison using a constant bat speed ( $\omega = 49$  rad/s) and a constant applied power (3.2 kW).

bat speed is controlled and likewise held constant. This trend will not be observed in play, however, where heavier bats are swung at slower speeds.

A more realistic basis for comparison would be to assume that the power available to accelerate the bat is constant. (A similar result is obtained assuming constant energy.) For the nominal case at hand ( $t = 3$  mm) 3.2 kW (4.3 hp) is required to accelerate the bat to 31 m/s in  $180^\circ$ . This same power was used to compute the swing speed of bats with thinner and thicker walls over the same  $180^\circ$  of rotation. The hit-ball speed from this constant power basis is also presented in Fig. 10 and shows a trend opposite from that found using constant bat swing speed. The trends presented in Fig. 10 clearly represent extreme variations in bat geometry. The results nevertheless indicate that current testing procedures may not represent a bat's true hitting response in play. Two bats can have the same length and weight, for instance, but differ in their inertia. Test procedures should account for a bat's inertia if a bat's response in play is to be accurately assessed.

A momentum balance of the bat and ball, before and after impact, may be expressed as

$$I\omega_1 + mv_p r = I\omega_2 + mv_h r, \quad (6)$$

where  $I$  is the mass moment of inertia of the bat about its center of rotation,  $\omega_1$  and  $\omega_2$  are the bat rotational velocities before and after impact, respectively,  $r$  is the distance from the impact location to the center of rotation,  $m$  is the mass of the ball, and  $v_p$  and  $v_h$  are the ball pitch and hit speeds, respectively. With swing speed and pitch speed specified, we have one equation with two unknowns. A second equation is obtained from the COR,  $e$ , as

$$e = \frac{\omega_2 r - v_h}{v_p - \omega_1 r}. \quad (7)$$

Using the momentum balance and the ball and bat speeds from the computational model, an effective COR may be computed. The COR is observed to vary by over a factor of three for the impact locations considered in Fig. 11. This is in contrast to the constant COR typically assumed when predicting hit speeds. (The total variation in the COR would be even larger if changes in relative speed as well as impact location were considered.) It should be noted that the COR is a measure of the system restoring energy to the ball. Impacts off the sweet spot, for instance, result in higher reaction forces, which generate larger bat deflections. This leads to more energy being absorbed by the bat and a decrease in the COR.

The sweet spot is usually defined as the impact location producing the highest hit-ball speed. There has been some discussion as to whether this location is located at the COP [15]. To determine the COP of the rotating bat numerically, the maximum reaction force at the center of rotation was plotted versus the impact location as shown in Fig. 12. For the unreinforced wooden bat, the reaction force was found to be minimum for an impact at 690 mm (27.2 in.) from the knob. The reaction force for the impact was not exactly equal to zero because of the vibration modes that were induced in the bat. The average period,  $T$ , was measured experimentally by suspending the bat about pivots at 75 mm (3 in.) from the knob end of the bat. The COP was then computed as [16]

$$\text{COP} = \frac{T^2 g}{4\pi^2}, \quad (8)$$

where  $g$  is the gravitational acceleration.

The COP was determined to be 675 mm (26.5 in.) from the knob end of the bat. While Eq. (8) assumes the bat center of rotation to lie along its length, the off-axis center of rotation used in the numerical model and bat machine should have a minimal effect on its COP location. Further

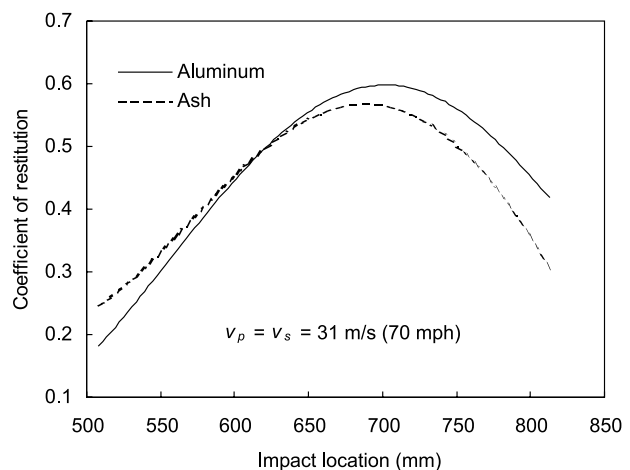


Fig. 11. Comparison of the coefficient of restitution for a wood and metal bat.

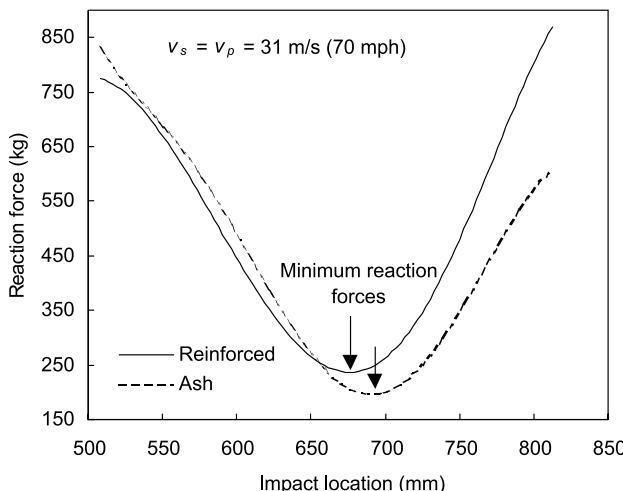


Fig. 12. Effect of reinforcement on the impact location producing the minimum reaction force.

Eq. (8) cannot explain the difference in the apparent COP of the wood and reinforced bats of Fig. 12. This places doubt on the reliability of using the classical COP to predict dynamic bat hitting characteristics. The importance of the ideal COP is placed in further question as the sweet spot is typically observed to be 5 mm to 25 mm (0.2–1 in.) outside of it, as shown in Figs. 6–8.

## 7. Summary

A finite element model has been used to predict the performance of hollow metal and solid wood bats. The model showed good agreement with the experimental data for bat performance and was used to study the influence of impact location, bat composition and impact velocities. The performance of aluminum bats was shown to depend on its wall thickness and the basis of comparison. A new basis for comparing bats with different inertia is proposed that uses a constant energy or power input, as opposed to the current practice of constant swing speed. A reinforcing strategy, intended to improve the durability of wood bats, was shown to have a negligible effect on hitting performance. The reinforced bat's reaction forces from ball impacts were noticeably different, however. These results raise questions concerning the usefulness of traditional bat performance metrics such as COP and dem-

onstrate the utility of computational techniques in the design process.

## Acknowledgements

This work has been funded by the Washington Technology Center and the Brett Brothers Bat Company. Their support is gratefully acknowledged.

## References

- [1] Bryant FO, Burkett LN, Chen SS, KrahenBuhl GS, Lu P. Dynamic and performance characteristics of baseball bats. *Rec Q Exerc Sport* 1979;48:505–10.
- [2] NCAA. Provisional Standard for Testing Baseball Bat Performance, 1999.
- [3] Trey Crisco, Personal communication, Brown University, 1999.
- [4] Wood Handbook. Wood as an engineering material. Forest Products Laboratory. Gen. Tech. Rep., FPL-GTR-113. US Department of Agriculture, Forest Service, Madison, WI.
- [5] Peters J. Experimental determination of properties of Northern White Ash. WMEL, WSU, 1999.
- [6] Dewey Chauvin, Personal communication, Easton Sports, 2000.
- [7] Tataro Y. On compression of rubber elastic sphere over a large range of displacements – Part 1. *J Eng Mater Technol* 1991;113/285.
- [8] Hermann LR, Peterson FE. A numerical procedure for viscoelastic stress analysis. In: Seventh Meeting of the ICRPG Mechanical Working Group, 1968; CPIA, Orlando, FL (Publication No. 177).
- [9] Smith LV, Shenoy M, Axtell JT. Simulated composite baseball bat impacts using numerical and experimental techniques. In: Proceedings of the Society of Experimental Mechanics, 2000; Orlando, FL, pp. 5–8.
- [10] Gibson RF. Principles of composite material mechanics. New York: McGraw-Hill; 1994.
- [11] Smith LV, Swanton SR. Response of braided composites under compressive loading. *J Compos Eng* 1993;312:1165–84.
- [12] Hughes TJR, Liu WK. Non-linear finite element analysis of shells – Part 2. Three-dimensional shells. *Comp Meths Appl Mech* 1981;27:331–362.
- [13] Shigley, Mischke. Mechanical engineering design. 5th ed. New York: Mc-GrawHill; 1989.
- [14] Axtell JT, Smith LV, Shenoy M. Effect of composite reinforcement on the durability of wood baseball bats. In: Proceedings of SAMPE, 2000; Boston MA, pp. 687–698.
- [15] Connolly WC, Cristian V. Locating the sweet spot. *Phy Educator* 1980;37:2123.
- [16] ASTM. F1881-98. Standard Test Method For Measuring Baseball Bat Performance Factor.